Medical & Biological Engineering & Computing (2018) 56:1077–1089
https://doi.org/10.1007/s11517-017-1752-5

ORIGINAL ARTICLE

Beat-to-beat estimation of stroke volume using impedance cardiography and artificial neural network

S. M. M. Naidu[1] · Prem C. Pandey[1] · Uttam R. Bagal[1] · Suhas P. Hardas[2]

Received: 15 July 2017 / Accepted: 3 November 2017 / Published online: 18 November 2017

Abstract
Impedance cardiography is a low-cost noninvasive technique, based on monitoring of the thoracic impedance, for estimation of stroke volume (SV). Impedance cardiogram (ICG) is the negative of the first derivative of the impedance signal. A technique for beat-to-beat SV estimation using impedance cardiography and artificial neural network (ANN) is proposed. A three-layer feed-forward ANN with error back-propagation algorithm is optimized by examining the effects of number of neurons in the hidden layer, activation function, training algorithm, and set of input parameters. The input parameters are obtained by automatic detection of the ICG characteristic points, and the target values are obtained by beat-to-beat SV measurements from time-aligned Doppler echocardiogram. The technique is evaluated using an ICG-echocardiography database with recordings from subjects with normal health in the under-rest and post-exercise conditions and from subjects with cardiovascular disorders in the under-rest condition. The proposed technique performed much better than the earlier established equation-based estimations, and it resulted in correlation coefficient of 0.93 for recordings from subjects with cardiovascular disorders. It may be helpful in improving the acceptability of impedance cardiography in clinical practice.

Keywords Artificial neural networks · Doppler echocardiography · Impedance cardiography · Stroke volume

1 Introduction

The time interval between two successive contractions of the heart is known as the cardiac cycle. Stroke volume (SV) is the amount of blood pumped out by the heart in one cardiac cycle. Cardiac output (CO) is the amount of blood pumped in 1 min and it is obtained as the product of SV and the heart rate [14]. SV and CO are important parameters for assessing the functioning of the cardiovascular system [20, 24, 29, 33, 43]. The established techniques for CO estimation are Fick's method, dye dilution, and thermodilution. These techniques are invasive and expensive and they are not usable for continuous SV monitoring [9, 40, 47]. The commonly used noninvasive technique is transthoracic echocardiography [4, 28, 38]. It requires expensive equipment and skilled manpower. Several studies have investigated SV variability and its relationship with respiration [10, 16, 17, 30]. Automatic beat-to-beat SV monitoring over an extended period using impedance cardiography can facilitate use of SV variability, like that of heart rate variability, for diagnosis of cardiovascular disorders.

Impedance cardiography is a low-cost noninvasive technique, based on monitoring of the thoracic impedance, for SV estimation [22, 25, 37, 39, 49]. It involves applying a low-level current (< 5 mA) of high frequency (20–100 kHz) through a pair of electrodes placed on the thorax and measuring the resulting amplitude-modulated voltage developed across another pair of electrodes placed inside the region bounded by the current injecting electrodes. The voltage is demodulated to get the signal proportional to the time-varying thoracic impedance, known as the impedance signal $Z(t)$. It comprises basal impedance Z_0 along with small time-varying component contributed by the variation in the blood volume in the thorax during the cardiac cycle and artifacts. Impedance cardiogram (ICG) is the negative of the first derivative of the impedance signal, i.e., $-dZ/dt$. Its landmarks associated with significant events in the cardiac cycle are known as the characteristic points [18, 26, 37, 45, 46]. These points are labeled as A, B, C, X, and O, as shown in an example of ICG along with simultaneously recorded electrocardiogram (ECG) in Fig. 1. Out of these points, the B, C, and X points

✉ Prem C. Pandey
pcpandey@ee.iitb.ac.in

[1] Department of Electrical Engineering, Indian Institute of Technology Bombay, Mumbai, Maharashtra 400076, India

[2] Hardas Heart Care, Shivajinagar, Pune, Maharashtra 411005, India

are used in most of the SV estimation methods. The C point is the peak in the ICG waveform during the systole and it is associated with the peak in the aortic blood velocity. The B point occurs, after the QRS complex in ECG, as a notch in the ICG waveform just before the rapid upstroke ascending towards the C point, and it is associated with the aortic valve opening. The lowest point after the C point is known as the X point and it is associated with the aortic valve closure. The C point is generally prominent and its detection is not significantly affected by respiratory and motion artifacts. The B point is often difficult to detect. It may be indistinct or may disappear in recordings with increased heart rate and its detection may get severely affected by artifacts [11, 36, 42].

Several equations for SV estimation, based on models of the thoracic impedance and the aortic blood flow profile, have been proposed [6, 25, 37, 41, 44, 49]. These equations use parameters obtained from impedance cardiography along with body-related parameters or empirically established scaling factors. The most commonly used parameters are the ICG peak, left ventricular ejection time measured as the B-X interval, basal impedance, distance between the voltage-measuring electrodes, blood resistivity, and the body-related physical parameters (height, weight, etc.). Several studies have compared the measurements using impedance cardiography with those using reference techniques like thermodilution and echocardiography [1, 2, 6, 8, 9, 12, 13, 19, 21, 23, 27, 28, 35, 45, 47–51]. Most of these studies involved subjects with normal health and some involved subjects with cardiovascular disorders. The results generally do not show a good agreement in the case of subjects with cardiovascular disorders. Assuming the estimation from the reference technique to be error-free, the disagreements could be due to errors in ICG parameters and inadequacies of the equations. Errors in estimation of the ICG parameters are caused by errors in detection of the characteristic points, presence of artifacts, and smearing of event latencies in ICG during ensemble averaging used for artifact suppression. The ICG parameter set and the model used for obtaining the equation may not be appropriate for SV estimation during cardiovascular disorders. Use of constants and parameters obtained from body-related measurements, as established through empirical studies on subjects with normal health, may introduce errors in the case of different disorders.

Considering the limitations of the methods based on models of the thoracic impedance and aortic blood flow profile, some researchers have proposed the use of artificial neural network (ANN) for SV estimation, assuming that the nonlinear relationship between SV and the ICG-related and other input parameters can be captured during the training of the network. Mulavara et al. [31] reported an ANN-based method for SV estimation with echocardiography as the reference technique. The study was conducted on recordings from 20 subjects with normal health, acquired in three supine body positions during six 5-s breath-hold durations separated by 15-s normal breathing. The cycles in each breath-hold duration were ensemble averaged and used to get the values of ICG peak, left ventricular ejection time, and heart rate. These values along with the inter-electrode distance, basal impedance, and volume of electrically participating thoracic tissues (calculated from height and weight) formed the set of inputs, and the SV values measured using echocardiography served as the target values. Half of the total 360 datasets (20 subjects, 3 positions, and 6 recordings) were used for training and the others for testing. They used a three-layer feed-forward network with hyperbolic tangent activation function in the hidden layer and error back propagation for training. Eight networks with different combination of inputs as used in the Kubicek and Sramek equations [25, 44] were evaluated.

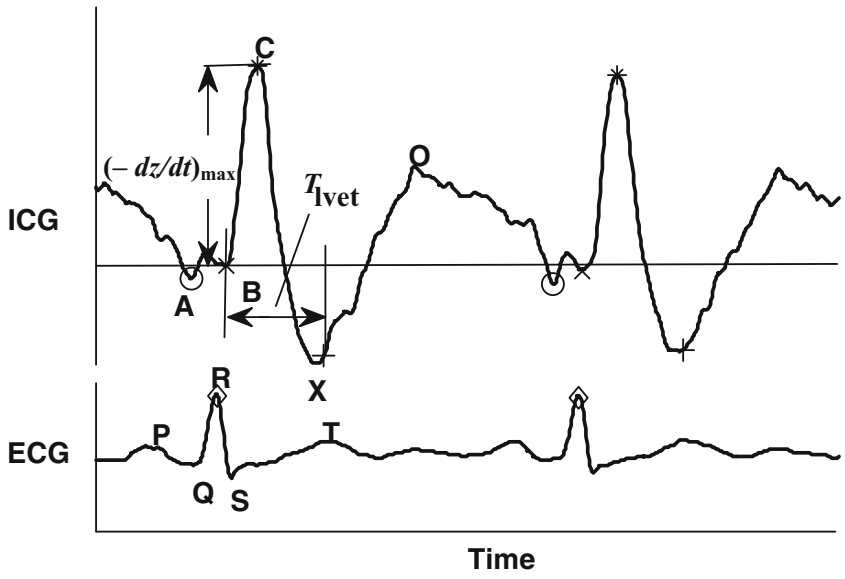

Fig. 1 An example of the ICG and ECG waveforms (recorded from a subject in the under-rest condition) with the corresponding characteristic points

Network with the superset of the inputs as used in the two equations and with five neurons in the hidden layer provided the best performance. Coefficients of determination for estimations using the Kubicek equation, the Sramek equation, and the ANN were 8.2, 9.9, and 77.4%, respectively, indicating the ANN-based estimation to be much better than the other two. Baura [5] described an ANN-based technique for noninvasive cardiac output monitoring using ICG parameters with thermodilution as the reference technique. It uses a three-layer feed-forward network, with three neurons in the hidden-layer and hyperbolic tangent activation function, trained using error back propagation. The inputs to the network comprise the heart rate, basal impedance, ICG peak, left ventricular ejection time, inter-electrode distance, and CO value as calculated by the Kubicek equation. Training of the network in this technique requires CO measurement on a large number of patients using thermodilution.

The earlier investigations on SV estimation used input parameters obtained from ensemble-averaged ICG and across-the-subjects training and testing. We propose an ANN-based method for SV estimation, with the ICG parameters from a large number of cycles without ensemble averaging as the inputs and the corresponding beat-to-beat SV values measured using echocardiography as the reference technique. For effectiveness of the ANN-based estimation, the datasets used for the training should be representative of the input-output relations as occurring in the datasets used for testing. Our approach assumes that the input-output relationships in the datasets from subjects with normal health with recordings under the conditions of the normal and increased heart rates can also be representative of the input-output relationships in the datasets from subjects with cardiovascular disorders. Echocardiography is used as the reference technique. It is noninvasive and it can be used for beat-to-beat SV estimation simultaneously along with impedance cardiography. The investigations are carried out using an ICG-echocardiography database with recordings from subjects with normal health in the under-rest condition and in the post-exercise condition with increased heart rate and from subjects with cardiovascular disorders in the under-rest condition.

2 Method

2.1 Signal recording and subjects

The ANN model is trained using the beat-to-beat values of SV estimated from Doppler echocardiography as the target values. Detection of ICG characteristic points for estimation of ICG parameters is carried out using R and T peaks of simultaneously recorded ECG. For this purpose, the ICG, ECG, and Doppler echocardiogram signals were simultaneously recorded in a clinical setting from a number of subjects in under-rest and post-exercise conditions.

The signals were recorded at Hardas Heart Care (Pune, Maharashtra, India), after approval of the protocol by the Ethics Committee of the hospital. The subjects were recruited, without gender and age balancing, from among the persons visiting the hospital for post-operative treatment, diagnosis, or health checkup. They were informed about the objectives of the study and the signal-recording procedure, and those willing to participate signed the consent. Participation did not involve any monetary benefit or cost for the subjects.

The subjects with normal health had no known history of cardiovascular disorders and were screened by a cardiologist on the basis of physical examination and ECG report. The subjects with cardiovascular disorders were the patients undergoing post-operative treatment or had a history of cardiovascular disorders. They were screened for suitability to participate in the study by the concerned cardiologist. The gender, age, height, and weight of the subjects were noted. The recordings were carried out over a period of 13 months. The group of subjects with normal health comprised 17 males and 1 female with age of 26–65 years (mean = 46.3 years, S.D. = 10.7 years), height of 1.54–1.80 m (mean = 1.69 m, S.D. = 0.06 m), and weight of 61–100 kg (mean = 76.2 kg, S.D. = 10.0 kg). The group of subjects with cardiovascular disorders had 19 males and 3 females with age of 24–78 years (mean = 51.5 years, S.D. = 15.8 years), height of 1.43–1.76 m (mean = 1.66 m, S.D. = 0.08 m), and weight of 52–97 kg (mean = 71.6 kg, S.D. = 11.7 kg).

The ICG signals were recorded using "HIC-2000 Impedance Cardiograph" from Bio-Impedance Technology (Chapel Hill, NC, USA). The impedance sensing was carried out using four-electrode configuration with Ag-AgCl disposable ECG spot electrodes. The outer two electrodes were used for injecting the excitation current and the resulting voltage was picked up across the inner two electrodes. The electrode placement is shown in Fig. 2. The upper current electrode was placed above the suprasternal notch on the front of the neck, with the lower one placed below the xiphoid process on the left lateral side of the thorax. The upper voltage electrode was placed at the base of the neck below the upper current electrode and the lower voltage electrode was placed at the level of xiphoid process on the left lateral side of the thorax above the lower current electrode. The distance between the voltage-sensing electrodes was noted. The instrument used 1 mA excitation current of 100 kHz and provided analog output signals corresponding to basal impedance (Z_0), deviation from basal impedance ($-z(t)$), and ICG ($-dZ/dt$)with the sensitivities of 40 mV/Ω, 0.5 V/Ω, and 400 mV/($\Omega \cdot s^{-1}$), respectively. It also provided analog ECG signal as sensed using the voltage electrodes. The output signals from the ICG instrument were acquired using the eight-channel, 12-bit signal acquisition module "KUSB-3102" from Keithley Instruments (Cleveland,

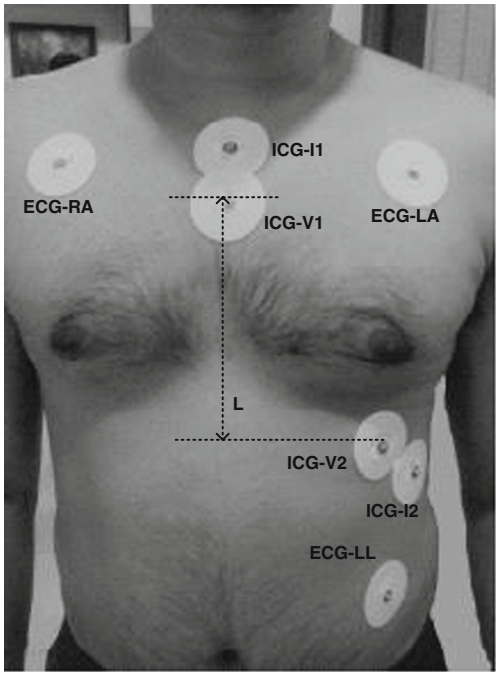

Fig. 2 Placement of electrodes on the chest: four ICG electrodes (current electrodes ICG-I1 and ICG-I2, voltage electrodes ICG-V1 and ICG-V2) and three ECG electrodes (ECG-RA, ECG-LA, and ECG-LL electrodes of ECG recorder of the echocardiography machine)

Ohio, USA) and connected through USB to a battery-powered notebook PC. The sampling frequency was set at 500 Hz.

The echocardiography recordings were carried out using "iE33 echocardiography system" from Philips Ultrasound (Bothell, WA, USA) with a 5-MHz phased-array probe placed on the chest after applying an ultrasound gel for good contact with the skin. The aortic blood velocity profile was recorded using apical five-chamber view of the ascending aorta. The aortic diameter was measured using parasternal long-axis view at the level of aortic annulus during mid-systole. The velocity-time integral (VTI) was estimated as the area between the envelope of the Doppler spectrum and its baseline with the help of the built-in software of the echocardiography machine by tracing the spectral envelope with its track ball. The ECG was recorded using the three-electrode ECG recorder of the echocardiography machine and displayed along with the Doppler echocardiogram. The ECG electrode positions are shown in Fig. 2 along with the ICG electrodes. As the recordings of ICG and Doppler echocardiogram waveforms employed independent time bases, the cardiac cycles of the two recordings were synchronized by alignment of the corresponding ECG-R peaks. An example of ICG and time-aligned Doppler echocardiogram is shown in Fig. 3.

For a subject with normal health, two recordings were carried out. The first recording was carried out with the subject relaxed, rested, and lying in the left-lateral position with a slight folding of the right leg. For the second recording, the subject underwent an exercise to increase the heart rate. The exercise was carried out, following the first four stages of the Bruce exercise protocol [7], for about 10 min on the "GE T-2100" treadmill from GE Healthcare (Wauwatosa, WI, USA) attached with "Smart Biphasic" defibrillator from Philips Healthcare (Andover, MA, USA). The signals were recorded soon after cessation of the exercise and with the subject lying the same way as for the first recording. The first and second sets of recordings are referred to as "under-rest" and "post-exercise" recordings. For a subject with cardiovascular disorder, only the under-rest recording was carried out. For all recordings, the subjects were advised to avoid any movements in order to minimize the motion artifacts, but no restrictions were placed on breathing. The recordings have been organized as a database and will be available for ICG-related research. The under-rest (UR) and post-exercise (PE) recordings from the 18 subjects with normal health (SNH) have 630 and 625 cardiac cycles, respectively, and these are referred to as the SNH-UR and SNH-PE recordings. These cycles pooled together resulted in 1255 cardiac cycles and are referred to as SNH-UR+PE. The under-rest recordings from the 22 subjects with cardiovascular disorders (SCD) have 842 cardiac cycles and these are referred to as the SCD-UR recordings.

2.2 ICG parameter extraction

The values of the basal impedance Z_0, the ICG peak $(-dZ/dt)_{\max}$, and the left ventricular ejection time T_{lvet} were obtained from impedance cardiography. Extraction of $(-dZ/dt)_{\max}$ and T_{lvet} requires detection of the B, C, and X points in the ICG waveform. The automatic beat-to-beat detection of these points was carried out using the technique reported by Naidu et al. [32]. In this technique, a wavelet-based denoising is employed for suppression of respiratory artifacts and beat-to-beat detection is carried out using multiple time-domain features of ICG, located with reference to R and T peaks of ECG, to reduce errors due to morphological variations. In each cycle, the ICG segment starting at the point corresponding to the R peak and duration equal to 35% of the R-R interval is scanned and the highest point is marked as the C point. The ICG segment preceding the C point and of duration equal to one fifth of the C-C interval is scanned, and the point with the lowest value is marked as the valley point. The difference between the values at the C point and the valley point is calculated as the peak-to-valley height H_{pv}. The first difference of the ICG is scanned backwards starting from the point corresponding to $0.3H_{pv}$ below the C point to the point corresponding to the valley point, and the point with change of sign is marked as the B point. If there is no sign change, the point $0.3H_{pv}$ above the valley point is marked as the B point. The ICG segment starting at the point corresponding to the T peak in ECG and duration equal to one third of the C-C interval is scanned, and the lowest point is marked as the X point. The

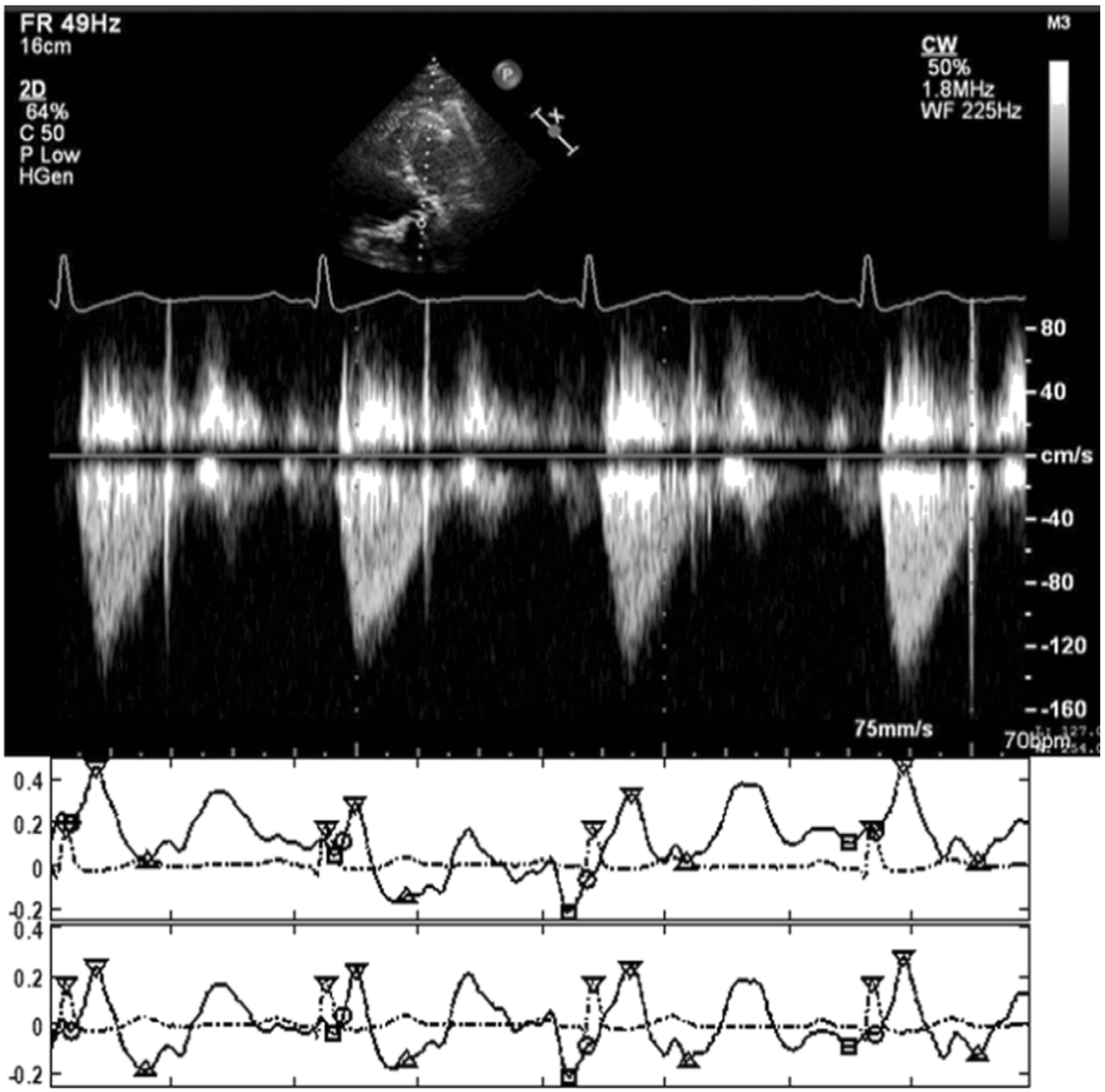

Fig. 3 An example of simultaneously recorded ICG and ECG with time-aligned Doppler echocardiogram (upper trace: blood velocity profile at aortic annulus with ECG as recorded by the echocardiography machine; middle trace: unprocessed ICG and simultaneously acquired ECG by the impedance cardiograph; lower trace: denoised ICG marked with the detected B, C, and X points and ECG marked with with R-peaks)

technique was evaluated using the ICG-echocardiography database [3]. The mean and standard deviation of the B-X intervals as measured by Doppler echocardiography (the intervals from the left ventricular valve opening to its closure) for all the cardiac cycles pooled together were 284 and 30 ms, respectively. The mean differences between the R-B, R-C, R-X, and B-X intervals as obtained from ICG and the corresponding intervals obtained by echocardiography were 2, 4, 26, and 24 ms, respectively. The corresponding standard deviations of differences were 22, 10, 48, and 54 ms.

The time interval from the B point to the X point in a cardiac cycle was taken as T_{lvet}. The height of the C point from the B point was taken as $(-dZ/dt)_{\max}$. Measuring the height of the C point from the B point and not from the baseline ($dZ/dt = 0$ line) helps in reducing error due to residual respiratory artifact. These values along with subject data were used as the inputs for SV estimation. The reference SV values were calculated as the product of VTI obtained from time-aligned Doppler echocardiogram and the cross-sectional area calculated from the measurement of aortic diameter at the annulus assuming circular cross-section, as described earlier as part of signal recording.

2.3 ANN model implementation, optimization, and testing

Designing the ANN model for an estimation application involves a careful selection of the network structure, training algorithm, the number of hidden layers and the number of neurons in each layer, the set of input parameters, pre-

processing of the input data, and criterion to stop training. It has been reported that a multi-layer feed-forward neural network with Levenberg-Marquardt or gradient-descent class of learning algorithm can track a nonlinear input-output relationship [34]. Normally, the number of neurons in the input layer is equal to the number of inputs in the parameter set and the hidden layer consists of an empirically determined optimal number of neurons with a nonlinear transfer function [15]. We have used a three-layer feed-forward ANN, with training using error back-propagation algorithm and nonlinear activation function in the hidden layer, for SV estimation. The network is shown in Fig. 4 for four inputs. The implementation was carried using MATLAB and Neural Network Toolbox Release 2013a (MathWorks, Inc.). The input parameters and the target values were transformed to have zero mean and unity variance to equalize their contributions in generalization of the model.

The training and testing of the network were carried out using two disjoint datasets, known as the training set and the testing set, respectively. The training set was partitioned into two disjoint subsets, with the datasets corresponding to two third of the randomly selected cardiac cycles assigned to the estimation set and the remaining ones assigned to the validation set. The weights of the network were initially set to random values. The estimation set was applied repeatedly for training of the network, and weight adjustment was carried out in batch mode on an epoch-by-epoch basis for improving the accuracy of the estimated output values with reference to the corresponding target values. The maximum number of epochs during training was set as 10,000. After each epoch, the validation set was used for checking the overfitting of the network. Increase in accuracy over the estimation set with the accuracy over the validation set remaining the same or decreasing was considered to be an indicator of overfitting and validation failure. The training was stopped in the case of 100 successive validation failures. Subsequently, the estimation capability of the trained network was assessed on the testing set.

The approximation error and the number of epochs for convergence depend on the training algorithm used for updating the weights [15, 34]. Out of the several training algorithms available in the Neural Network Toolbox (MathWorks), nine commonly used ones were used for implementing the networks: Broyden-Fletcher-Goldfarb-Shanno (BFGS) quasi-Newton, Polak-Ribiére conjugate gradient, scaled conjugate gradient, one-step secant, resilient back propagation, conjugate gradient with Powell-Beale restarts, variable learning rate back propagation, Fletcher-Powell conjugate gradient, and Levenberg-Marquardt.

The commonly used ICG parameters in the different equation-based methods for SV estimation are inter-electrode distance L, basal impedance Z_0, ICG peak $(-dZ/dt)_{max}$, and left ventricular ejection time T_{lvet}, or transformations and combinations of these parameters. We have used these parameters along with the R-R interval as the inputs. In addition to them, the subject's age, height, and weight were also used as the inputs. Several variations of the network, differing in terms of the number of neurons in the hidden layer, activation function in the hidden layer, and training algorithm for updating the weights were used to find a near-optimal network. Subsequently, four investigations were carried out for optimizing the network by examining the effect of varying one aspect of the network at a time while keeping the other aspects fixed: (i) number of neurons in the hidden layer, (ii) activation function, (iii) training algorithm, and (iv) set of input parameters.

The investigations for optimizing the network were carried out using the datasets corresponding to the SNH-UR and SNH-PE recordings from subjects with normal health pooled together, referred to as SNH-UR+PE. These datasets were partitioned into two disjoint sets, with the datasets corresponding to 60%

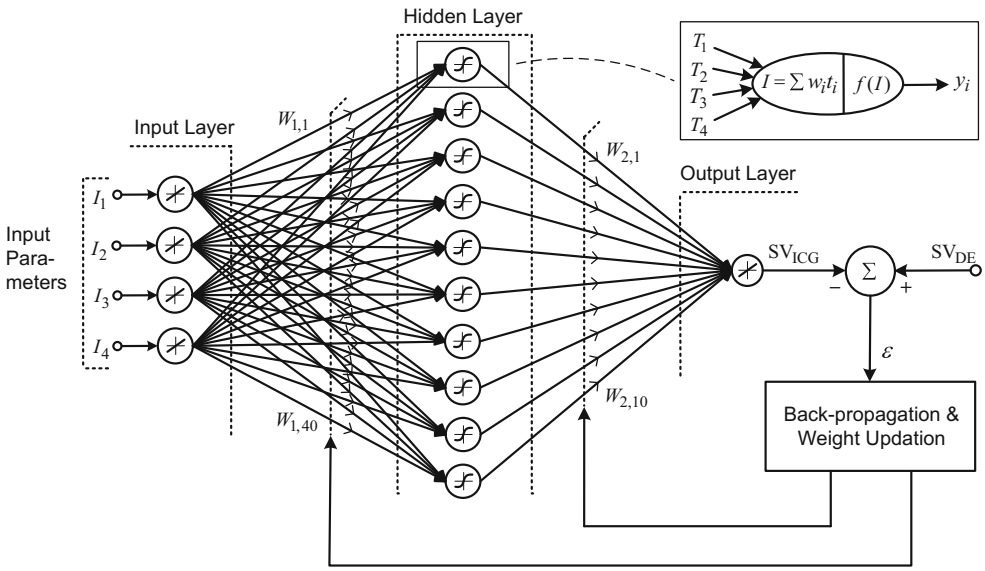

Fig. 4 A three-layer feed-forward ANN, with training using error back-propagation algorithm and nonlinear activation function in the hidden layer, for SV estimation

of the randomly selected cardiac cycles assigned to the training set and the remaining 40% assigned to the testing set.

The optimal network as selected on the basis of the results of the earlier four investigations was used for examining the effect of different datasets for training. The training was carried out using training sets obtained from the SNH-UR, SNH-PE, and SNH-UR+PE datasets, resulting in three trained networks. Each of these networks was tested on the testing sets obtained from SNH-UR, SNH-PE, and SNH-UR+PE datasets. In each case, the training set comprised randomly selected 60% of the cardiac cycles with the remaining 40% used as the testing set. The three networks were subsequently tested on SCD-UR with 100% of the cardiac cycles used as the testing set.

Performances of the three networks were compared with estimations using the Kubicek, Sramek, and Bernstein equations [6, 25, 44] as the following:

$$\mathrm{SV}_{Kubicek} = \rho \frac{L^2}{Z_0^2} \left(-\frac{dZ}{dt} \right)_{\max} T_{lvet} \tag{1}$$

$$\mathrm{SV}_{Sram\ ek} = \frac{(0.17H)^3}{4.25} \frac{(-dZ/dt)_{\max}}{Z_0} T_{lvet} \tag{2}$$

$$\mathrm{SV}_{Bernstein} = \frac{16W^{1.02}}{\zeta^2} \sqrt{(-dZ/dt)_{\max}/Z_0}\, T_{lvet} \tag{3}$$

In the Kubicek equation, ρ is the blood resistivity and its value was taken as 150 Ω - m. In the Sramek equation, $H$is the subject height. In the Bernstein equation, SV in milliliters is calculated using Z_0 in Ω, $(-dZ/dt)_{\max}$ in $\Omega \cdot \mathrm{s}^{-1}$, T_{lvet} in s, and body weight W in kg, and index of transthoracic conduction ζ calculated as:

$$\zeta = \begin{cases} \left(Z_C^2 - Z_C Z_0\right) / \left(2Z_C^2 + Z_0^2 - 3Z_C Z_0\right), & Z_0 < Z_C \\ 1, & Z_0 < Z_C \end{cases}$$

with the critical impedance Z_C (taken empirically as 20 Ω).

3 Results

3.1 Selection of the optimal network

For selection of the optimal network, the under-rest and post-exercise recordings from subjects with normal health were pooled together, resulting in 1255 cardiac cycles with the mean and standard deviation of the SV values as 86.3 and 18.8 mL, respectively. As described earlier, the training set comprised 60% of randomly selected cycles, i.e., there were 753 cycles in the training set and remaining 502 cycles in the testing set. The training set was further partitioned into estimation set with 502 cycles (2/3 of the training set) and validation set with remaining 251 cycles. The network was implemented with eight input parameters: L, Z_0, $(-dZ/dt)_{\max}$, T_{lvet}, RR (R-R interval from ECG), age, Ht (height), and Wt (weight). Investigations were carried out for examining the effects of (i) number of neurons in the hidden layer, (ii) activation function, (iii) training algorithm for updating the weights, and (iv) set of input parameters.

Performance comparison was carried out by tabulating the number of epochs for convergence during training and mean error $\overline{\varepsilon}$, standard deviation of errors σ_ε, and correlation coefficient r with reference to the target values for the testing sets. In selecting the optimal network, the number of epochs for convergence is given lower precedence than the error-related performance indices.

For examining the effect of the number of neurons in the hidden layer, the hyperbolic-tangent function was selected as the activation function and the Levenberg-Marquardt algorithm was selected for updating the weights. The performance indices for the number of hidden-layer neurons that varied from 3 to 20 are given in Table 1. The network with three-neuron hidden layer needed the largest number of epochs for training. The $\overline{\varepsilon}$ values were small (< 1 mL) in all cases. On the basis of values of σ_ε and r, the networks with eight or more neurons may be considered to have better performance than those with three or five neurons and the network with 10 neurons may be considered to be optimal.

The effect of different activation functions was examined for the network with the 10-neuron hidden layer and the Levenberg-Marquardt algorithm for updating the weights. The networks were implemented with three activation functions: radial basis, logistic, and hyperbolic tangent. The results are given in Table 2. The number of epochs was smallest for the radial basis function. The $\overline{\varepsilon}$ values were small (< 1 mL) in all cases. The hyperbolic-tangent function had smallest σ_ε values and hence it may be considered to be the optimal choice although it had a somewhat larger number of epochs than the other two functions.

Table 1 Effect of different number of neurons in the ANN hidden layer (activation function: hyperbolic tangent, training algorithm: Levenberg-Marquardt). Number of cardiac cycles in the testing set = 502. N_{epoch} number of epochs for training, $\overline{\varepsilon}$ mean error, σ_ε standard deviation of errors, r correlation coefficient

No. of neurons	N_{epoch}	$\overline{\varepsilon}$ (mL)	σ_e (mL)	r
3	177	0.29	9.16	0.880
5	18	− 1.14	7.64	0.924
8	31	− 0.14	6.38	0.944
10	66	0.42	6.06	0.947
13	29	− 0.45	7.06	0.934
15	39	0.55	6.90	0.937
20	10	− 0.47	7.26	0.931

$p < 0.0001$ for all r values

Table 2 Effect of different activation functions used in the ANN hidden layer (number of hidden-layer neurons: 10, training algorithm: Levenberg-Marquardt). Number of cardiac cycles in the testing set = 502. N_{epoch} number of epochs for training, $\overline{\varepsilon}$ mean error, σ_ε standard deviation of errors, r correlation coefficient

Activation function	N_{epoch}	$\overline{\varepsilon}$ (mL)	σ_e (mL)	r
Radial basis	19	− 0.16	6.33	0.942
Logistic	30	− 0.56	6.22	0.952
Hyperbolic tangent	66	0.42	6.06	0.947

Effect of different training algorithms was examined on the network with 10 neurons in the hidden layer and the hyperbolic tangent as the activation function. The results are given in Table 3. All algorithms resulted in small $\overline{\varepsilon}$ values (< 1.5 mL) and the variation in performance of different algorithms in terms of σ_ε and r was small. There was a large variation in the number of epochs for different algorithms. It was smallest for Levenberg-Marquardt algorithm and much lower than that for other algorithms. This algorithm also resulted in nearly the smallest σ_ε and highest r, and hence it may be considered as the optimal choice for our application.

The investigations for examining the effect of number of neurons in the hidden layer, activation function, and training algorithm showed the network with 10-neuron hidden layer, hyperbolic tangent activation function, and Levenberg-Marquardt training algorithm to be the optimal choice. This network was used for investigating the contribution of different non-ICG parameters by excluding them in different combinations. The results of training and testing of the networks are given in Table 4. The exclusion of different input parameters had a large effect on the number of epochs, with range of 14–417. The $\overline{\varepsilon}$ values were small (< 1.5 mL) in all cases, the σ_ε values ranged 6.1–11.8 mL, and the r values ranged 0.819–0.950. Small number of epochs was associated with large σ_ε values in most cases and hence cannot be used by itself as an indicator for comparing the importance of the parameters. Cases with small σ_ε values were generally associated with high r values.

Network with exclusion of none of the input parameter had 66 epochs and smallest σ_ε. Among single-parameter exclusions, RR exclusion resulted in largest σ_ε indicating its importance. Among two-parameter exclusions, [RR, age] exclusion had largest σ_ε. Among three-parameter exclusions, largest σ_ε was observed for [age, Ht, Wt] exclusion indicating that these parameters were collectively important although not individually. Exclusion of all the non-ICG parameters together had largest number of epochs and largest σ_ε, thus indicating collective importance of these parameters for improving the speed of convergence and decreasing the error in SV estimation. Therefore, it may be inferred that the four non-ICG parameters are needed for the optimal network and the R-R interval is the most important one out of these parameters.

Table 3 Effect of different ANN training algorithms (number of hidden-layer neurons: 10, activation function: hyperbolic tangent). Number of cardiac cycles in the testing set = 502. Algorithms: BFGS (BFGS quasi-Newton), PRCG (Polak-Ribiére conjugate gradient), SCG (scaled conjugate gradient), OSS (one step secant), RBP (resilient back-propagation), CGPB (conjugate gradient with Powell-Beale restarts), VLRB (variable learning rate back-propagation), FPCG (Fletcher-Powell conjugate gradient), LM (Levenberg-Marquardt). N_{epoch} number of epochs for training, $\overline{\varepsilon}$ mean error, σ_ε standard deviation of errors, r correlation coefficient

Algorithm	N_{epoch}	$\overline{\varepsilon}$ (mL)	σ_e (mL)	r
BFGS	9999	− 0.64	6.55	0.947
PRCG	2621	− 0.85	6.35	0.951
SCG	2030	0.34	6.90	0.929
OSS	892	0.79	7.97	0.914
RBP	668	− 0.81	7.24	0.922
CGPB	2383	− 0.86	7.47	0.927
VLRB	9925	− 1.46	7.20	0.924
FPCG	1623	0.09	6.24	0.946
LM	66	0.42	6.06	0.947

$p < 0.0001$ for all r values

Table 4 Effect of exclusion of different non-ICG parameters (number of hidden-layer neurons: 10, activation function: hyperbolic tangent, training algorithm: Levenberg-Marquardt). Number of cardiac cycles in the testing set = 502. N_{epoch} number of epochs for training, $\overline{\varepsilon}$ mean error, σ_ε standard deviation of errors, r correlation coefficient

Excluded parameter(s)	N_{epoch}	$\overline{\varepsilon}$ (mL)	σ_e (mL)	r
None	66	0.42	6.06	0.947
Ht	51	− 0.10	6.74	0.939
Wt	62	− 0.43	6.78	0.950
Age	205	0.45	6.79	0.938
RR	27	1.08	7.10	0.919
Ht, Wt	37	0.63	6.96	0.932
Ht, age	148	0.07	6.62	0.942
Ht, RR	147	0.24	7.49	0.906
Wt, age	213	− 0.07	7.31	0.941
Wt, RR	14	1.00	7.86	0.905
Age, RR	162	0.56	7.91	0.915
Ht, Wt, age	36	1.27	9.15	0.878
Ht, Wt, RR	92	− 0.09	8.33	0.895
Ht, age, RR	77	− 0.11	8.12	0.908
Wt, age, RR	30	0.86	8.23	0.909
Ht, Wt, age, RR	417	0.41	11.81	0.819

$p < 0.0001$ for all r values

3.2 Comparison of ANN and equation-based methods

Based on the results of the investigations presented in the previous subsection, ANN with eight inputs (L, Z_0, $(-dZ/dt)_{max}$, T_{lvet}, RR, age, Ht, Wt), 10 neurons in the hidden layer, hyperbolic tangent activation function, and Levenberg-Marquardt training algorithm was selected as the optimal network for beat-to-beat SV estimation. Further investigation was carried out to examine the performance of this network for different combinations of the training and testing sets and for comparing its performance with equation-based estimations. In the subsequent description, the networks trained on training sets with the SNH-UR, SNH-PE, and SNH-UR+PE datasets are referred to as ANN1, ANN2, and ANN3, respectively. The Kubicek, Sramek, and Bernstein equations are referred to as EQKB, EQSR, and EQBR, respectively. The performance comparisons of the ANN-based and the equation-based estimations were carried out for the testing sets corresponding to the SNH-UR, SNH-PE, SNH-UR+PE, and SCD-UR datasets.

The results are summarized in Table 5. Results for the three trained networks ANN1, ANN2, and ANN3 show that the performance of each trained network was best when the training and testing sets corresponded to the same datasets, with almost similar pattern for the three performance indices. The network ANN3 resulted in $\bar{\varepsilon} = 0.1$ mL, $\sigma_\varepsilon = 6.6$ mL, and $r = 0.95$ for SNH-UR+PE. The performance of ANN1 on SNH-UR and that of ANN2 on SNH-PE were almost similar. However, the performance of ANN1 on SNH-PE and SNH-UR+PE and that of ANN2 on SNH-UR and SNH-UR+PE were significantly poor. The performance of ANN3 on SNH-UR and SNH-PE was almost similar to that on SNH-UR+PE. These results indicate that training of the network on the pooled data significantly improved its performance and that ANN3 can be used for SV estimation on all three SNH datasets. Testing of ANN3 on SCD-UR resulted in $\bar{\varepsilon} = -0.1$ mL, $\sigma_\varepsilon = 7.2$ mL, and $r = 0.93$, showing only a slight performance degradation compared to its testing on SNH-UR+PE. Testing of ANN1 and ANN2 on SCD-UR gave relatively poor results. These results show that training of the optimal network on the training set obtained by pooling of the under-rest and post-exercise recordings from the subjects with normal health enabled the network for SV estimation on recordings from subjects with cardiovascular disorders.

As seen in Table 5, the three equation-based SV estimations resulted in relatively large $\bar{\varepsilon}$, large σ_ε, and low r values for all the four testing sets. The performance of the Bernstein equation (EQBR) was generally better than that of the other two equations. This equation resulted in $\bar{\varepsilon} = -38.0$ mL, $\sigma_\varepsilon = 48.7$ mL, and $r = 0.36$ for testing on SNH-UR+PE and in $\bar{\varepsilon} = -44.8$ mL, $\sigma_\varepsilon = 40.9$ mL, and $r = 0.33$ for testing on SCD-UR. Thus, the ANN-based method, particularly with the training set obtained by pooling of the under-rest and post-exercise recordings from subjects with normal health, may be considered to be much more effective than the equation-based methods for beat-to-beat SV estimation from subjects with normal health as well as those with cardiovascular disorders.

Figure 5 gives plots of difference of estimations versus mean of estimations (Bland-Altman plots) for beat-to-beat SV estimations using impedance cardiography with ANN3 and Doppler echocardiography for the SNH-UR+PE and SCD-UR datasets, showing the distribution of differences along with 95% confidence interval ($\bar{\varepsilon} \pm 1.96\sigma_\varepsilon$). The plots show that the distribution of differences between the two

Table 5 Comparison of the ANN-based and equation-based beat-to-beat SV estimations: mean error ($\bar{\varepsilon}$), standard deviation of errors (σ_e), and correlation coefficient (r) with reference to the SV values obtained using Doppler echocardiography

Testing set (N = No. of cardiac cycles)	Perform. index	Estimation method					
		ANN1	ANN2	ANN3	EQKB	EQSR	EQBR
SNH-UR ($N = 252$)	$\bar{\varepsilon}$ (mL)	0.37	−5.62	−0.39	−52.70	−52.31	−42.03
	σ_e (mL)	5.99	31.19	5.95	30.29	30.97	32.14
	r	0.950	0.716	0.951	0.154	0.198	0.265
SNH-PE ($N = 250$)	$\bar{\varepsilon}$ (mL)	5.79	−0.16	0.90	−42.13	−49.33	−33.68
	σ_e (mL)	15.23	7.43	7.17	56.84	34.07	40.02
	r	0.752	0.930	0.936	0.210	0.228	0.291
SNH-UR+PE ($N = 502$)	$\bar{\varepsilon}$ (mL)	3.04	−2.15	0.07	−47.09	−50.77	−37.98
	σ_e (mL)	12.65	14.30	6.59	46.23	32.61	48.73
	r	0.773	0.725	0.946	0.363	0.295	0.364
SCD-UR ($N = 842$)	$\bar{\varepsilon}$ (mL)	1.36	−2.21	−0.10	−42.08	−38.21	−44.84
	σ_e (mL)	9.30	9.71	7.20	37.67	35.65	40.88
	r	0.829	0.812	0.933	0.292	0.163	0.329

$p < 0.0001$ for all r values

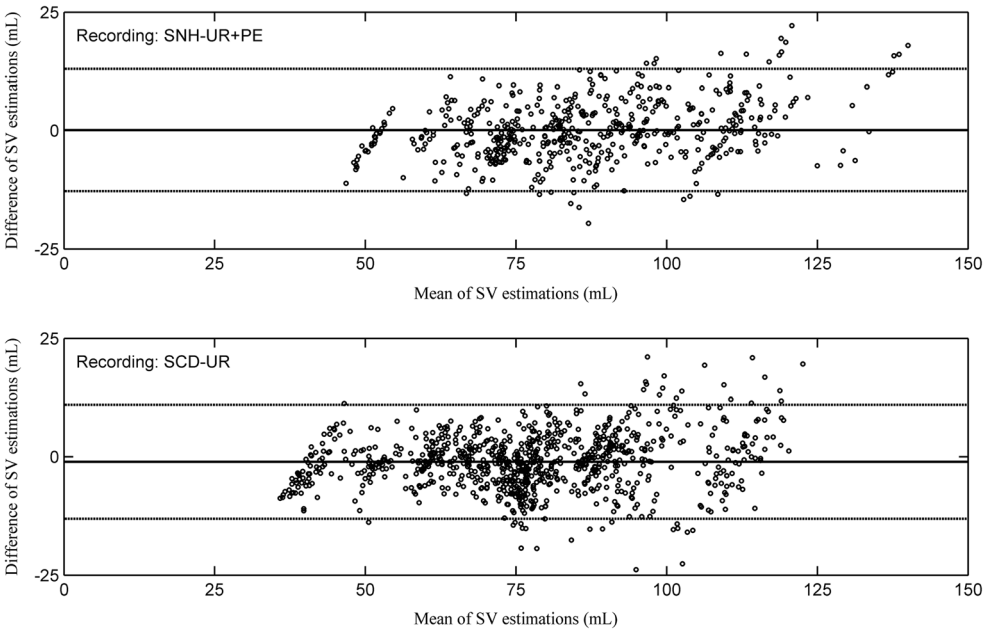

Fig. 5 Bland-Altman plots of beat-to-beat SV estimation (mL) using ANN3 on the SNH-UR+PE and SCD-UR recordings with the SV values measured from Doppler echocardiogram as reference (solid line: $\overline{\varepsilon}$, dotted lines: $\overline{\varepsilon} \pm 1.96\sigma_{\varepsilon}$)

measurement techniques are similar for both the datasets, indicating that the performance of ANN3 for recordings from the subjects with cardiovascular disorders is similar to that for recordings from the subjects with normal health. There is an increase in the error at the higher SV values, which may be due to sparsity of training data at this end.

Earlier studies [2, 8, 12, 31, 35, 48] on evaluation of impedance cardiography with reference to Doppler echocardiography for SV estimation have used estimation over a set of cycles for each subject. In the study by Mulavara et al. [31] using ANN-based SV estimation on subjects with normal health, the correlation coefficients for estimations using the Kubicek equation, the Sramek equation, and the ANN-based method were 0.29, 0.32, and 0.88, respectively. For comparison with such studies, the beat-to-beat SV estimations in our study were evaluated for average of SV values across the cardiac cycles for each of the 22 subjects with cardiovascular disorders. All three equation-based estimations resulted in large $\overline{\varepsilon}$ and σ_{ε} values, and low r values, with $\overline{\varepsilon} = -43.1$ mL, $\sigma_{\varepsilon} = 43.5$ mL, and $r = 0.20$ for EQBR. The ANN-based estimations resulted in much lower $\overline{\varepsilon}$ and σ_{ε}values, and larger r values, with $\overline{\varepsilon} = 0.4$ mL, $\sigma_{\varepsilon} = 5.7$ mL, and $r = 0.96$ for ANN3. Thus, the ANN-based estimation outperformed the equation-based estimation for beat-to-beat variation as well as for average SV estimation.

4 Discussion

An ANN-based technique for beat-to-beat SV estimation has been proposed and investigated using an ICG-echocardiography database. The ICG parameters are obtained using a technique for automatic detection of the B, C, and X points. Our approach assumes that the input-output relationships in the datasets from subjects with normal health, with the recordings in the under-rest condition and in the post-exercise condition after the heart rate has been increased by participation of the subject in the Bruce exercise protocol, can also be representative of the input-output relationships in the datasets from subjects with cardiovascular disorders. A three-layer feed-forward network with error back-propagation algorithm was selected for SV estimation. The network was implemented for eight input parameters: inter-electrode distance, basal impedance, ICG peak, left ventricular ejection time, R-R interval, age, height, and weight. Three of these parameters (ICG peak, left ventricular ejection time, and R-R interval) are estimated on beat-to-beat basis and the other five parameters are subject-dependent. The input parameters and the target values were transformed to equalize their contributions in generalization of the model. The investigations were carried out in two stages. The first stage involved optimization of the network by examining the effects of number of neurons in the hidden layer, activation function, and training algorithm for updating the weights, and set of input parameters. The second stage involved testing of the network by examining the effect of different combinations of training and testing sets and comparison with equation-based estimations.

The investigations for optimizing the network were carried out using the datasets from the subjects with normal health with the under-rest and post-exercise recordings pooled together. These investigations showed that the best performance was obtained with the network with 10-neuron hidden layer, hyperbolic tangent activation function, and Levenberg-Marquardt training algorithm. Exclusion of the four non-ICG parameters (R-R interval, age, height, and weight) in different combinations showed that R-R interval was

important in decreasing the error and the combination of height, weight, and age together helped in significantly decreasing the number of epochs needed for convergence during training and also the errors. Therefore, it may be inferred that the four non-ICG parameters have an important role in ANN-based SV estimation. These parameters were retained as part of the inputs for the second stage of the investigation.

The second stage of investigation involved examining the effect of different combinations of training and testing sets on performance of the optimal network and comparing its performance with equation-based estimations. Three network models were developed by using three types of training sets from the recordings from the subjects with normal health: (i) under rest, (ii) post exercise, and (iii) under rest and post exercise pooled together. All the three trained networks were tested using the three testing sets. Results showed that the performance of each trained network was best when the training and testing sets corresponded to the same datasets. Performance of the first two networks degraded when tested on different datasets. Performance of the third network did not degrade for testing on the other two types of datasets. Therefore, this network may be considered as better than the other two.

Performances of the trained networks were compared with three established equation-based methods, for the recordings from the subjects with normal health and for recordings from the subjects with cardiovascular disorders. In comparison with the ANN-based estimations, the equation-based estimations had poor performance on all indicators. The Bernstein equation generally performed better than the other two equations. It provided correlation coefficients of 0.36 and 0.33 for the recordings from the subjects with normal health and for subjects with cardiovascular disorders, respectively. The corresponding values for the best ANN-based estimation were 0.95 and 0.93. The Bland-Altman plots showed the distribution of errors in the ANN-based SV estimation for recordings from the subjects with cardiovascular disorders to be similar to that for recordings from the subjects with normal health.

For a comparison of the results with earlier studies [2, 8, 12, 31, 35, 48], the beat-to-beat SV estimations were averaged over the cardiac cycles for each subject. The correlation coefficients for the equation-based estimations were low and similar to those reported in earlier studies. The correlation coefficient for ANN-based estimation was 0.96 and higher than the earlier reported values.

Thus, the results show that the ANN-based estimation with training using the pooled datasets from the subjects with normal health can be used for different datasets and pooling is needed for training to extend the use of the trained network for SV estimation for the subjects with cardiovascular disorders. The results further show that the proposed method is usable for measuring SV averaged over a set of cardiac cycles and for beat-to-beat SV monitoring.

Investigations need to be carried out with a larger database. Training data from a larger number of subjects and particularly with higher levels of exercise can help in reducing sparsity of datasets at the ends of the SV range and in improving the effectiveness of ANN-based estimation. The testing needs to be carried out with a larger number of subjects with cardiovascular disorders. Use of other types of networks and techniques for detection of ICG characteristic points with smaller errors should be investigated. Use of the C-C interval in place of the R-R interval in the input parameter set may be helpful in further improving the performance. Effects of inclusion of additional ICG parameters, such as B-C interval, C-X interval, and ICG value at the X point, need to be investigated.

5 Conclusion

It may be concluded that the proposed ANN-based technique using the optimized network and the ICG parameters obtained by automatic beat-to-beat detection of the B, C, and X points and the beat-to-beat R-R interval can be used for SV estimation for subjects with normal health and cardiovascular disorders. Its performance is better than the equation-based estimations and it provides estimation with low bias and high precision. Investigations using other types of networks, larger database, technique for detection of ICG characteristic points with smaller errors, and use of additional ICG parameters may be helpful in further improving its performance. The technique may be helpful in improving the acceptability of impedance cardiography for use in clinical practice.

Acknowledgements The authors are thankful to Dr. Niranjan D Khambete and Dr. Vinayak N Desurkar of Deenanath Mangeshkar Hospital and Research Center, Pune, India, for preliminary recordings for this study and many insightful discussions.

Compliance with ethical standards All procedures involving human participation were in accordance with the ethical standards of the institutional and/or national research committee and with the 1964 Helsinki Declaration and its later amendments or comparable ethical standards.

Conflict of interest The authors declare that they have no conflict of interest.

References

1. Arora D, Chand R, Mehta Y, Trehan N (2007) Cardiac output estimation after off-pump coronary artery bypass: a comparison of two different techniques. Ann Card Anaesth 10(2):132–136
2. Aust PE, Belz GG, Belz G, Koch W (1982) Comparison of impedance cardiography and echocardiography for measurement of stroke volume. Eur J Clin Pharmacol 23(6):475–477
3. Bagal UR, Pandey PC, Naidu SMM, Hardas SP (2017) Detection of opening and closing of the aortic valve using impedance

cardiography and its validation by echocardiography. Biomed Physics Eng Express. https://doi.org/10.1088/2057-1976/aa8bf5
4. Baumgartner H, Hung J, Bermejo J, Chambers JB, Evangelista A, Griffin BP, Iung B, Otto CM, Pellikka PA, Quiñones M (2009) Echocardiographic assessment of valve stenosis: EAE/ASE recommendations for clinical practice. Eur J Echocardiography 10:1–25
5. Baura GD (2001) Noninvasive continuous cardiac output monitor US Patent No US 6186955 B1
6. Bernstein DP, Lemmens HJM (2005) Stroke volume equation for impedance cardiography. Med Biol Eng Comput 43(4):443–450
7. Bruce RA, Lovejoy FW Jr, Pearson R, PNG Y, Brothers GB, Velasquez T (1949) Normal respiratory and circulatory pathways of adaptation in exercise. J Clin Invest 28(6 Pt 2):1423–1430
8. Castor G, Klocke RK, Stoll M, Helms J, Niedermark I (1994) Simultaneous measurement of cardiac output by thermodilution, thoracic electrical bioimpedance and Doppler ultrasound. Br J Anaesth 72(1):133–138
9. De Maria AN, Raisinghani A (2000) Comparative overview of cardiac output measurement methods: has impedance cardiography come of age? Congest Heart Fail 6(2):60–73
10. Elstad M, Walloe L (2015) Heart rate variability and stroke volume variability to detect central hypovolemia during spontaneous breathing and supported ventilation in young, healthy volunteers. Physiol Meas 36(4):671–681
11. Ermishkin VV, Kolesnikov VA, Lukoshkova EV (2014) Age-dependent and pathologic changes in ICG waveforms resulting from superposition of pre-ejection and ejection waves. Physiol Meas 35(6):943–963
12. Fellahi JL, Caille V, Charron C, Deschamps-Berger PH, Vieillard-Baron A (2009) Noninvasive assessment of cardiac index in healthy volunteers: a comparison between thoracic impedance cardiography and Doppler echocardiography. Anesth Analg 108(5):1553–1559
13. Fortin J et al (2006) Non-invasive beat-to-beat cardiac output monitoring by an improved method of transthoracic bioimpedance measurement. Comp Biol Med 36(11):1185–1203
14. Guyton AC, Hall JE (2006) Textbook of medical physiology, 11th edn. Saunders, Elsevier
15. Haykin S (1999) Neural networks: a comprehensive foundation, 2nd edn, Prentice Hall, Upper Saddle River
16. Hoff IE, Hoiseth LO, Hisdal J, Roislien J, Landsverk SA, Kirkeboen KA (2014) Respiratory variations in pulse pressure reflect central hypovolemia during noninvasive positive pressure ventilation. Crit Care Res Pract 2014:9. https://doi.org/10.1155/2014/712728
17. Holme NL, Rein EB, Elstad M (2016) Cardiac stroke volume variability measured non-invasively by three methods for detection of central hypovolemia in healthy humans. Eur J Appl Physiol 116(11–12):2187–2196
18. Hurwitz BE, Shyu L-Y, Reddy SP, Schneiderman N, Nagel JH (1990) Coherent ensemble averaging techniques for impedance cardiography. In: Proc 3rd Ann IEEE Symp CBMS, Chapel Hill, pp 228–235
19. Jensen L, Yakimets J, Teo KK (1995) A review of impedance cardiography. Heart & Lung: J Acute Crit Care 24(3):183–193
20. Kerr AJ, Simmonds MB, Stewart RA (1998) Influence of heart rate on stroke volume variability in atrial fibrillation in patients with normal and impaired left ventricular function. Am J Cardiol 82(12):1496–1500
21. Kieback AG, Borges AC, Schink T, Baumann G, Laule M (2010) Impedance cardiography versus invasive measurements of stroke volume index in patients with chronic heart failure. Int J Cardiol 143(2):211–213
22. Kim DW (1989) Detection of physiological events by impedance. Yonsei Med J 30(1):1–11
23. Kizakevich PN, Teague SM, Nissman DB, Jochem WJ, Niclou R, Sharma MK (1993) Comparative measures of systolic ejection during treadmill exercise by impedance cardiography and Doppler echocardiography. Biol Psychol 36(1–2):51–61
24. Korhonen I, Koobi T, Turjanmaa V (1999) Beat-to-beat variability of stroke volume measured by whole-body impedance cardiography. Med Biol Eng Comput 37(Suppl.1):61–62
25. Kubicek WG, Kottke FJ, Ramos MU, Patterson RP, Witsoe DA, Labree JW, Remole W, Layman TE, Schoening H, Garamela JT (1974) The Minnesota impedance cardiograph theory and applications. Biomed Eng 9(9):410–416
26. Lababidi Z, Ehmke DA, Durnin RE, Leaverton PE, Lauer RM (1970) The first derivative thoracic impedance cardiogram. Circulation 41(4):651–658
27. Lababidi Z, Ehmke DA, Durnin RE, Leaverton PE, Lauer RM (1971) Evaluation of impedance cardiac output in children. Pediatrics 47(5):870–879
28. Lewis JF, Kuo LC, Nelson JG, Limacher MC, Quinones MA (1984) Pulsed Doppler echocardiographic determination of stroke volume and cardiac output: clinical validation of two new methods using the apical window. Circulation 70(3):425–431
29. Liu H, Yambe T, Sasada H, Nanka S, Tanaka S, Nagatomi R, Nitta S (2004) Comparison of heart rate variability and stroke volume variability. Auton Neurosci 116(1–2):69–75
30. Marik PE, Cavallazzi R, Vasu T, Hirani A (2009) Dynamic changes in arterial waveform derived variables and fluid responsiveness in mechanically ventilated patients: a systematic review of the literature. Crit Care Med 37(9):2642–2647
31. Mulavara AP, Timmons WD, Nair MS, Gupta V, Kumar AA, Taylor BC (1998) Electrical impedance cardiography using artificial neural networks. Ann Biomed Eng 26(4):577–583
32. Naidu SMM, Bagal UR, Pandey PC, Hardas S, Khambete ND (2014) Detection of characterisitc points of impedance cardiogram and validation using Doppler echocardiography. In Proc 11th Ann Conference of the IEEE India Council (Indicon 2014), Pune, India, doi: https://doi.org/10.1109/INDICON.2014.7030596
33. Nelson N, Janerot-Sjoberg B (2001) Beat-to-beat changes in stroke volume precede the general circulatory effects of mechanical ventilation: a case report. Crit Care 5(1):41–45
34. Nocedal J, Wright SJ (1999) Nonlinear least-squares problems. In: Glynn P, Robinson SM (eds) Numerical Optimization. Springer, New York, pp 262–266
35. Northridge DB, Findlay IN, Wilson J, Henderson E, Dargie HJ (1990) Non-invasive determination of cardiac output by Doppler echocardiography and electrical bioimpedance. Br Heart J 63(2):93–97
36. Ono T, Miyamura M, Yasuda Y, Ito T, Saito T, Ishiguro T, Yoshizawa M, Yambe T (2004) Beat-to-beat evaluation of systolic time intervals during bicycle exercise using impedance cardiography. Tohoku J Exp Med 203(1):17–29
37. Patterson RP (1989) Fundamentals of impedance cardiography. IEEE Eng Med Biol Mag 8(1):35–38
38. Peterson GE, Brickner ME, Reimold SC (2003) Transesophageal echocardiography: clinical indications and applications. Circulation 107(19):2398–2402
39. Qu M, Zhang Y, Webster JG, Tompkins WJ (1986) Motion artifact from spot and band electrodes during impedance cardiography. IEEE Trans Biomed Eng 33(11):1029–1036
40. Scherhag A, Kaden JJ, Kentschke E, Sueselbeck T, Borggrefe M (2005) Comparison of impedance cardiography and thermodilution-derived measurements of stroke volume and cardiac output at rest and during exercise testing. Cardiovasc Drugs Ther 19(2):141–147
41. Sherwood A, Allen MT, Fahrenberg J, Kelsey RM, Lovallo WR, van Doornen LJ (1990) Methodological guidelines for impedance cardiography. Psychophysiology 27(1):1–23

42. Sherwood A, McFetridge J, Hutcheson JS (1998) Ambulatory impedance cardiography: a feasibility study. J Appl Physiol 85(6): 2365–2369
43. Siebert J, Drabik P, Lango R, Szyndler K (2004) Stroke volume variability and heart rate power spectrum in relation to posture changes in healthy subjects. Med Sci Monit 10(2):MT31–MT37
44. Sramek B (1984) Noninvasive continuous cardiac output monitor. US Patent 4450527
45. Summers RL, Shoemaker WC, Peacock WF, Ander DS, Coleman TG (2003) Bench to bedside: electrophysiologic and clinical principles of noninvasive hemodynamic monitoring using impedance cardiography. Acad Emerg Med 10(6):669–680
46. Takada K, Fujinami T, Senda K, Nakayama K, Nakano S (1977) Clinical study of 'A waves' (atrial waves) in impedance cardiograms. Am Heart J 94(6):710–717
47. Tang WH, Tong W (2009) Measuring impedance in congestive heart failure: current options and clinical applications. Am Heart J 157(3):402–411
48. van der Meer NJ, Noordegraaf AV, Kamp O, De Vries PM (1999) Noninvasive measurement of cardiac output: two methods compared in patients with mitral regurgitation. Angiology 50(2):95–101
49. Van De Water JM, Miller TW, Vogel RL, Mount BE, Dalton ML (2003) Impedance cardiography: the next vital sign technology? Chest 123(6):2028–2033
50. Wang XA, Sun HH, Adamson D, Van de Water JM (1989) An impedance cardiography system: a new design. Ann Biomed Eng 17(5):535–556
51. Woltjer HH, Bogaard HJ, Scheffer GJ, van der Spoel HI, Huybregts MA, de Vries PM (1996) Standardization of non-invasive impedance cardiography for assessment of stroke volume: comparison with thermodilution. Br J Anaesth 77(6):748–752

S. M. M. Naidu received the degrees of BTech in electronics and instrumentation from Andhra University (India) in 2001 and MTech in electrical engineering with specialization in control and instrumentation from Motilal Nehru National Institute of Technology, Allahabad (India) in 2005. He is an associate professor at Koneru Lakshmaiah University, Guntur (India), and concurrently pursuing PhD at IIT Bombay (India). His research interests include biomedical instrumentation and signal processing.

Prem C. Pandey received the degrees of BTech in electronics engineering from Banaras Hindu University (India) in 1979, MTech in electrical engineering from IIT Kanpur (India) in 1981, and PhD in electrical and biomedical engineering from the University of Toronto (Canada) in 1987. In 1987, he joined the University of Wyoming (USA) as an assistant professor and later joined IIT Bombay (India) in 1989, where he is a professor in electrical engineering. His research interests include speech and signal processing, biomedical signal processing and instrumentation, and embedded system design.

Uttam R. Bagal received the degrees of BSc (Tech) in electronic instrumentation from Mumbai University (India) in 1992 and MTech in biomedical engineering from IIT Bombay (India) in 2000. He is an assistant professor at the MGM College of Engineering and Technology, Navi Mumbai (India), and is concurrently pursuing PhD at IIT Bombay (India). His research interests include biomedical instrumentation and signal processing.

Suhas P. Hardas received the degrees of MBBS and MD in general medicine from Pune University (India) in 1985 and 1990, respectively, and DM in cardiology from Mumbai University (India) in 1994. He has held a number of clinical, teaching, and research positions in the areas of interventional cardiology and electrophysiology at hospitals in Australia, India, Saudi Arabia, and USA. He is director of cardiology at Poona Hospital and Research Center, Pune (India) since 2013. He is a practicing interventional cardiologist with research interests in echocardiography and electrophysiology.